MOLECULAR AND CELLULAR BIOLOGY, Mar. 2009, p. 1442–1451 Vol. 29, No. 6
0270-7306/09/$08.00+0 doi:10.1128/MCB.01689-08

Auto- and Cross-Regulation of the hnRNP L Proteins by Alternative Splicing▽‡

Oliver Rossbach,[1]† Lee-Hsueh Hung,[1]† Silke Schreiner,[1]† Inna Grishina,[1] Monika Heiner,[1] Jingyi Hui,[2] and Albrecht Bindereif[1]*

Institute of Biochemistry, Justus Liebig University of Giessen, Heinrich-Buff-Ring 58, D-35392 Giessen, Germany,[1] and State Key Laboratory of Molecular Biology, Institute of Biochemistry and Cell Biology, Shanghai Institutes for Biological Sciences, Chinese Academy of Sciences, Yue-Yang Road 320, Shanghai 200031, People's Republic of China[2]

Received 31 October 2008/Returned for modification 8 December 2008/Accepted 23 December 2008

We recently characterized human hnRNP L as a global regulator of alternative splicing, binding to CA-repeat and CA-rich elements. Here we report that hnRNP L autoregulates its own expression on the level of alternative splicing. Intron 6 of the human hnRNP L gene contains a short exon that, if used, introduces a premature termination codon, resulting in nonsense-mediated decay (NMD). This "poison exon" is preceded by a highly conserved CA-rich cluster extending over 800 nucleotides that binds hnRNP L and functions as an unusually extended, intronic enhancer, promoting inclusion of the poison exon. As a result, excess hnRNP L activates NMD of its own mRNA, thereby creating a negative autoregulatory feedback loop and contributing to homeostasis of hnRNP L levels. We present experimental evidence for this mechanism, based on NMD inactivation, hnRNP L binding assays, and hnRNP L-dependent alternative splicing of heterologous constructs. In addition, we demonstrate that hnRNP L cross-regulates inclusion of an analogous poison exon in the hnRNP L-like pre-mRNA, which explains the reciprocal expression of the two closely related hnRNP L proteins.

Alternative splicing regulation provides a major mechanism for increasing diversity of gene expression and mediating tissue and developmental control in higher eukaryotes. For many years, studies have focused on mechanisms and factors for a few model genes, but more recently genome-wide approaches have yielded additional insight into the complexity of alternative splicing regulation. Currently, genomewide models attempt to describe networks of relatively few global splicing regulators that act on many target genes in a combinatorial manner. It is often more than a single factor that determines a specific alternative splicing process. These splicing-regulatory networks can be viewed as one of several layers of gene regulation, embedded in other networks such as those of transcription, miRNA-mediated regulation, nonsense-mediated decay (NMD), polyadenylation, translation, or cellular localization (1–3, 6, 21, 25, 34, 36). Most splicing regulators characterized thus far belong to either one of two groups, the family of serine-arginine-rich (SR) proteins and the heterogeneous nuclear ribonucleoproteins (hnRNPs).

We have focused for the last few years on hnRNP L, an abundant nuclear, multifunctional RNA-binding protein with four RNA-recognition motifs (29) that plays both nuclear and cytoplasmic roles in mRNA export of intronless genes (9, 18), IRES-mediated translation (10), mRNA stability (11, 14, 33), and splicing (see below). We have recently characterized in more detail its RNA-binding specificity and function as a global alternative splicing regulator (13, 16). Initial evidence for hnRNP L's splicing-regulatory role came from a single human gene, coding for endothelial nitric oxide synthase, which contains in its intron 13 a polymorphic CA repeat region where hnRNP L binds and acts as a splice activator (15). Based on a SELEX-derived consensus for hnRNP L RNA binding, CA-repeat, and certain CA-rich motifs, we identified and characterized a small number of other targets in the human genome (13), which was recently expanded through a splice-sensitive microarray/RNAi strategy (16). In sum, from intronic positions hnRNP L can act either as an activator or repressor in diverse alternative splicing decisions, apparently depending on splice site proximity. In addition, exonic regulatory sites are known for hnRNP L, best characterized in the case of the *CD45* variable exons, where hnRNP L modulates exon repression during T-cell activation (12, 23, 30). In addition to hnRNP L, a closely related protein, hnRNP L-like (hnRNP LL), has been described (16, 35), and recent evidence points to a specific role of hnRNP LL in alternative splicing regulation of CD45 and other target genes during T-cell activation (27, 38).

Several recent studies have pointed out NMD-mediated RNA degradation as an important element in alternative splicing regulation, although its genomewide impact is still controversial (e.g., see reference 28). One classical splice regulator, the repressor protein PTB (for polypyrimidine tract binding protein), has been studied in detail. It is autoregulated by a negative-feedback loop on the alternative splicing level, involving PTB-dependent exon 11 skipping, which induces NMD; thereby, excess PTB protein levels are effectively downregulated (37, 40). This auto- and cross-regulatory network be-

* Corresponding author. Mailing address: Institute of Biochemistry, Justus-Liebig-University of Giessen, Heinrich-Buff-Ring 58, D-35392 Giessen, Germany. Phone: 49-641-9935 420. Fax: 49-641-9935 419. E-mail: albrecht.bindereif@chemie.bio.uni-giessen.de.

† O.R., L.-H.H., and S.S. contributed equally to this study.

‡ Supplemental material for this article may be found at http://mcb.asm.org/.

▽ Published ahead of print on 5 January 2009.

tween PTB and its paralog nPTB operates not only through NMD and alternative splicing but also involves control by a tissue-specific microRNA (4, 20; reviewed in references 7 and 19; see also Discussion).

Steven Brenner's group discovered that, surprisingly, every member of the entire SR-protein family of regulators contains ultraconserved nucleotide sequences in their respective pre-mRNAs that coincide with NMD-relevant alternative splicing (17). This new concept and correlation between alternative splicing-mediated NMD and ultraconserved sequence holds also for many hnRNP proteins and was suggested to represent a general mechanism often utilized by RNA-binding proteins for maintaining homeostasis of their protein levels (26, 31). However, the underlying autoregulatory mechanisms remained largely unclear in their detail, although this is of great general interest, since they might yield new insight into the intriguing and unsolved question why extended intronic sequences might be ultraconserved.

While searching for alternatively spliced hnRNP L target genes, we noted that the hnRNP L pre-mRNA itself contains in its intron 6 a very unusual, long CA-rich cluster and a short, alternatively spliced poison exon; in addition, this entire region of ~2 kb in intron 6 is highly conserved, close to ultraconservation in the strict sense. We demonstrate here that the CA-cluster functions as an hnRNP L-dependent activator of poison exon 6A inclusion and that the paralog hnRNP LL pre-mRNA contains a corresponding poison exon, which is cross-regulated by hnRNP L. These auto- and cross-regulatory relationships in the hnRNP L/LL system give new insight into homeostatic control and the role of ultraconserved intronic sequences in gene regulation.

MATERIALS AND METHODS

Oligonucleotides. For sequences of DNA oligonucleotides, see the supplemental material.

Cycloheximide treatment, small interfering RNA (siRNA) knockdown, and RNA analysis. For inhibition of translation and NMD, Dulbecco modified Eagle medium (Invitrogen) containing 50 μg of cycloheximide/μl was added to a confluent culture of HeLa cells. Cell aliquots were harvested before cycloheximide addition (time point zero) and after addition at the time points indicated, followed by RNA isolation (TRIzol reagent; Invitrogen). Reverse transcription-PCR (RT-PCR) was performed by using Expand RT enzyme (Roche) and the primers L exon 6 fwd and L exon 7 rev according to the manufacturer's protocol, followed by analysis on 2% agarose gels and ethidium bromide staining. As DNA size markers, the Gene Ruler DNA ladder mix (Fermentas) was used.

One day before siRNA transfection, HeLa cells were seeded on 10-cm culture dishes (4.3×10^5 cells per dish). siRNA duplex (at a final concentration in culture medium of 30 nM) was transfected with Lipofectamine 2000 (Invitrogen) according to the manufacturer's instructions. The siRNA duplexes specific for human hnRNP L, human UPF1, and luciferase GL2 were as follows: human hnRNP L H1, 5′-GAA UGG AGU UCA GGC GAU GdTdT-3′ (MWG Biotech); human UPF1, 5′-GAU GCA GUU CCG CUC CAU UdTdT-3′ (Sigma); and luciferase GL2, 5′-CGU ACG CGG AAU ACU UCG ATT-3′ (MWG Biotech).

Four days after siRNA transfection, knockdown efficiencies were assessed by Western blotting with monoclonal antibodies against hnRNP L (4D11; Sigma) and, as controls, γ-tubulin (GTU-88; Sigma) and GAPDH (glyceraldehyde-3-phosphate dehydrogenase; Ambion). As indicated, cycloheximide treatment was done (at a final concentration of 50 μg/ml) before the cells were harvested, for up to 4 h after RNA interference (RNAi) knockdown; the efficiency of UPF1 knockdown was measured by Western blotting with anti-UPF1 antibody (8). If necessary, protein bands were quantitated by TINA software, version 2.07d.

Total RNA was isolated by using TRIzol (Invitrogen) and an RNeasy kit (Qiagen). Total RNA (1 μg) was reverse transcribed, using an iScript cDNA synthesis kit (Bio-Rad) according to the manufacturer's instructions, followed by PCR with the primers L exon 6 fwd and L exon 7 rev (see above). Real-time PCR assays (16) for hnRNP L and β-actin mRNAs were performed in an iCycler (Bio-Rad), using a SYBR green Jumpstart *Taq* Readymix kit (Bio-Rad), the primer pairs β-actin fwd/rev, or exon-specific hnRNP L or LL primer pairs (L exon 2 fwd/L exon 3 rev; L exon 4 fwd/L exon 5 rev; L exon 6A fwd/L exon 7 rev; L exon 7 fwd/L exon 8 rev; L exon 8 fwd/L exon 10 rev; LL exon 6 fwd/LL exon 7 rev).

hnRNP L overexpression constructs. (i) hnRNP L-His. The EcoRI-PstI restriction fragment containing the full-length cDNA for hnRNP L was released from pRSET hnRNP L (10) and cloned into pcDNA3 vector, resulting in pcDNA3-hnRNP L. The hnRNP L open reading frame was recloned into TOPO vector pcDNA3.1/V5-His-TOPO (Invitrogen), according to the manufacturer's instructions, resulting in pcDNA3.1/hnRNP L-V5-His, which carries a C-terminal V5-His tag.

(ii) hnRNP L-GST. The full-length cDNA for hnRNP L, together with the open reading frame of the glutathione *S*-transferase (GST) tag, was released from the plasmid pFASTBAC HTb-hnRNP L-GST (13) by BamHI digestion. This fragment was cloned into pcDNA3 vector (Invitrogen), resulting in pcDNA3-hnRNP L-GST.

One day before transfection, HeLa cells were seeded in 10-cm culture dishes. Cells were transfected at 80% confluence with 10 μg of DNA (His- or GST-hnRNP L), according to the manufacturer's instructions (FuGENE HD transfection reagent; Roche). For the mock transfection, pcDNA3.1 DNA was used. Cells were harvested 2 days after transfection and analyzed by Western blotting with monoclonal antibodies against hnRNP L (4D11; Sigma) and γ-tubulin (GTU-88; Sigma). Protein bands were quantitated by using TINA software, version 2.07d.

hnRNP L (or LL)-RNA binding analysis by biotin-RNA pull-down assay. The 5′ and 3′ parts of the CA-rich cluster of hnRNP L intron 6 were amplified from human genomic DNA and cloned in the pCR2.1-TOPO vector (Invitrogen) to give plasmid pCR2.1-TOPO-5′-CA (nucleotides [nt] −1005 to −716 of intron 6) and pCR2.1-TOPO-3′-CA (nt −491 to −156), respectively (see Fig. S1 in the supplemental material for the intron 6 sequence). An unrelated control sequence (327 nt) was PCR amplified from pCR2.1-TOPO DNA, using the primers FP-T7-cluster-delta and RP-cluster-delta.

Template DNAs for in vitro transcription (MEGAshortscript kit; Ambion) of 5′-CA (300-nt) and 3′-CA (346-nt) clusters, as well as nonspecific control sequence (327 nt), were PCR amplified from these constructs, introducing the T7 promoter, followed by chemical 3′-end biotinylation (39). 3′-biotinylated RNAs or 5′-biotinylated $(CA)_{32}$ RNA (2 μg of each) were incubated in a final volume of 225 μl at room temperature for 30 min with 25 μl of HeLa nuclear extract in RP-50 buffer (50 mM KCl, 1 mM $MgCl_2$, 10 mM HEPES [pH 7.5]) containing 10 mM dithiothreitol, 100 μg of tRNA/ml, and 10 U of RNaseOUT (Invitrogen). Then, 40 μl of packed NeutrAvidin agarose beads (Thermo Scientific) was added, and incubation was continued at room temperature for 20 min. After precipitation and four washes with RP-70 buffer (70 mM KCl, 1 mM $MgCl_2$, 10 mM dithiothreitol, 10 mM HEPES [pH 7.5]), bound protein was released by sodium dodecyl sulfate (SDS) sample buffer (2% SDS, 80 mM Tris-HCl, 5% β-mercaptoethanol, 15% glycerol, 0.05% bromophenol blue [pH 6.8]) and incubation at 95°C for 5 min and then analyzed by SDS-polyacrylamide gel electrophoresis (10% polyacrylamide gel) and Western blotting with monoclonal anti-hnRNP L antibody (4D11; Sigma) or anti-hnRNP LL antibody (16).

In vitro splicing. T7-DUP 3′CA-cluster-6A and control 6A constructs (three exons)—684 bp of intron 6 of the human hnRNP L gene (535 bp containing the 3′ CA cluster, exon 6a, and 79 bp of intron 6a)—were PCR amplified using human genomic DNA (kindly provided by Karl Stangl, Charité, Berlin, Germany) and the primers L intron 6 fwd and L intron 6a. Products were cloned into the β-globin-derived pDUP4.1 (24) in between the ApaI and BglII sites, thereby replacing the middle DUP exon. For the control construct lacking the CA-rich cluster, only 270 bp of the hnRNP L region were cloned into pDUP4.1 as described above, using the primers Δcluster_fwd and i6a_rev. This region contained the 70-bp exon 6A and 121 bp of upstream and 79 bp of downstream intronic sequence. An nonspecific sequence without any high-score hnRNP L binding motifs, which was PCR amplified from a noncoding region of pCR2.1-TOPO vector using the primers sub_fwd and sub_rev, was inserted into the ApaI site. In addition, a double-stranded oligonucleotide of 60 bp, derived from the hnRNP L intron 6 and containing a putative distant branch point and made by annealing the oligonucleotides BPins-sense and BPins-antisense, was cloned into the BglII site of the substituting sequence.

To prevent usage of cryptic splice sites and to assure proper RT-PCR analysis, the following modifications were included. First, in both constructs the β-globin part of the upstream intron was shortened by 41 bp through a two-step mutagenesis PCR, in the first step with the primer combinations txc_fwd/DUPmut_rev (5′

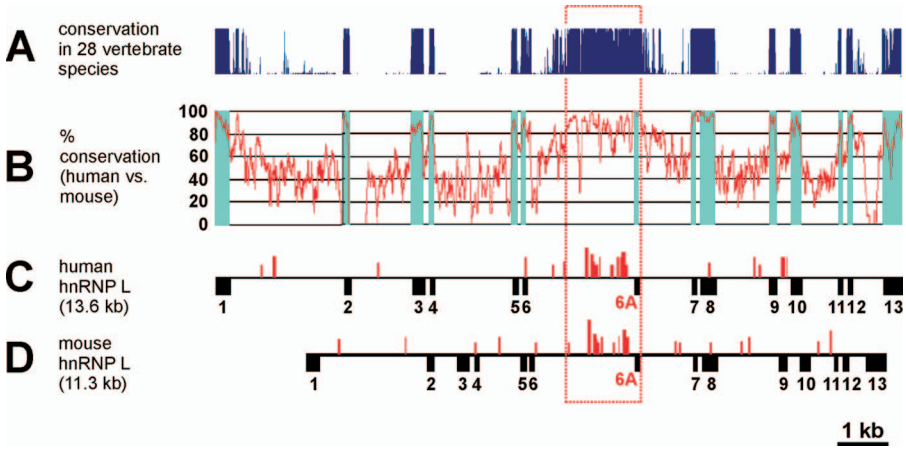

FIG. 1. Exon-intron structure, nucleotide sequence conservation, and map of CA-rich elements in the hnRNP L gene. (A and B) Nucleotide sequence conservation is diagrammed for the hnRNP L gene from 28 vertebrate species (UCSC Genome browser; http://genome.ucsc.edu/) (A) and by comparing human versus mouse sequences, plotting percentage of identity over 50-nt windows across the gene (B). Blue regions indicate the 13 exons; the highly conserved region in intron 6 is circled in red. (C and D) Exon-intron structure of human (C) and mouse (D) hnRNP L genes. Above the line, red bars represent hnRNP L binding motifs, with their height corresponding to their score (for how these scores were derived, see reference 16).

fragment) and DUPmut-B_fwd or DUPmut-sub_fwd, respectively, and txc_rev primer (3′ fragment) and in the second step with the primers txc_fwd and txc_rev. PCR products were cloned into pCR2.1-TOPO vector (Invitrogen). Second, a cryptic 5′ splice site located in the downstream intron was removed by deleting the GT dinucleotide by two-step mutagenesis PCR, using the primers txc_fwd and mut-css_rev, as well as mut-css_fwd and txc_rev in the first step and the primers txc_fwd and txc_rev in the second step, followed by recloning into pCR2.1-TOPO as described previously.

HeLa cell nuclear extract was depleted of hnRNP L by incubation with a biotinylated $(CA)_{32}$ RNA oligonucleotide and neutravidin-agarose beads (15). Depletion was confirmed by Western blotting with hnRNP L antibodies (4D11; Sigma) and GAPDH antibodies (Ambion) as a loading control.

m^7GpppG-capped RNAs were transcribed in vitro from PCR products as templates. For the three-exon pre-mRNA, the primers txc_fwd and txc_rev were used; for the two-exon pre-mRNA, the primers txc_fwd and i6a_rev were used; and for the pre-mRNAs with the mutated exon 6a 5′ splice, the primers 5'ss-wt_rev and 5'ss-mut_rev, respectively, were used. In vitro splicing assays were performed in HeLa nuclear extract (CIL Biotech, Belgium), incubating 5 ng of pre-mRNA per 12.5-μl reaction mixture, as described previously (15). Splicing was monitored by RT-PCR, with the respective reverse primers used for transcription and the forward primers DUP1_fwd or DUP5_fwd, followed by analysis on 2% agarose gels and ethidium bromide staining.

Transfection and RNA analysis. To investigate CA-cluster-dependent splicing in vivo, hnRNP L-exon 6a-minigene constructs were cloned in between the EcoRI and XbaI sites of the pcDNA3.1 vector. A total of 6×10^5 HeLa cells were seeded on a 6-cm dish the day before transfection. Cells were transfected by the calcium phosphate method (32). After 3 days, cells were harvested, and total RNA was isolated by guanidinium isothiocyanate and treated with RQ1-DNase (Promega). After reverse transcription (iScript cDNA synthesis kit; Bio-Rad) PCR was carried out, using the primers DUP5_fwd and BGH_rev. Products were analyzed as described above.

RESULTS

Highly conserved region in the hnRNP L gene contains intronic CA-rich cluster and NMD-sensitive exon 6A. Analyzing the exon-intron structure and sequence conservation of hnRNP L genes from 28 vertebrate species (http://genome.ucsc.edu/), we noted an extended region of ~2 kb, located in the middle of the 3.3-kb intron 6, which represents the most highly conserved region in the entire hnRNP L gene (Fig. 1, see boxed region). For example, the human and mouse nucleotide sequences exhibit 87% identity in this region (Fig. 1B; see also Fig. S1 in the supplemental material for a sequence alignment). Intron 6 contains a short exon, which we have termed 6A; it is not part of the RefSeq mRNA and is documented only through several cDNAs (AK301062 and AK298384). If included, exon 6A would introduce a premature termination codon, expected to induce NMD.

When we searched for hnRNP L binding sites in the hnRNP L pre-mRNA sequence, we were surprised to find a dense cluster of high-score hnRNP L binding motifs extending over more than 800 nt within this highly conserved intronic region (see Fig. 1C and D for the human and mouse genes; here, potential hnRNP L binding sites are graphically represented by red bars, with their heights indicating motif scores and their widths reflecting the positions and lengths of the motifs, based on a scoring system) (16). In sum, this suggests that hnRNP L may bind to its own pre-mRNA in this highly conserved part of intron 6, regulating inclusion of the poison exon 6A.

We next tested whether exon 6A inclusion induces NMD by treating HeLa cell cultures with cycloheximide, inhibiting translation and thereby NMD, followed by measuring exon 6A inclusion by RT-PCR and an exon 6-7 primer pair (Fig. 2A). Alternatively to cycloheximide treatment, UPF1, an essential component of the NMD machinery, was downregulated by RNAi (to 48% relative to the γ-tubulin control [see Fig. 2B]). First, cycloheximide treatment over 3 h resulted in a strong increase of exon 6A usage, from initially 22% to levels of 47% relative to the major exon 6-7 spliced form; as a control, alternative splicing of exon 20 of the *TJP1* pre-mRNA, another hnRNP L target, was not affected (Fig. 2A). Second, the inclusion of poison exon 6A increased from almost undetectable levels in the control luciferase knockdown (4%) to 34% after UPF1 knockdown (Fig. 2B and C). In sum, the novel exon 6A, which we identified within an extended highly conserved intron 6 region, represents an NMD target and is preceded by an unusual, long CA-rich cluster.

hnRNP L binds to conserved CA-rich cluster. We predicted that hnRNP L protein binds with high affinity to the intronic

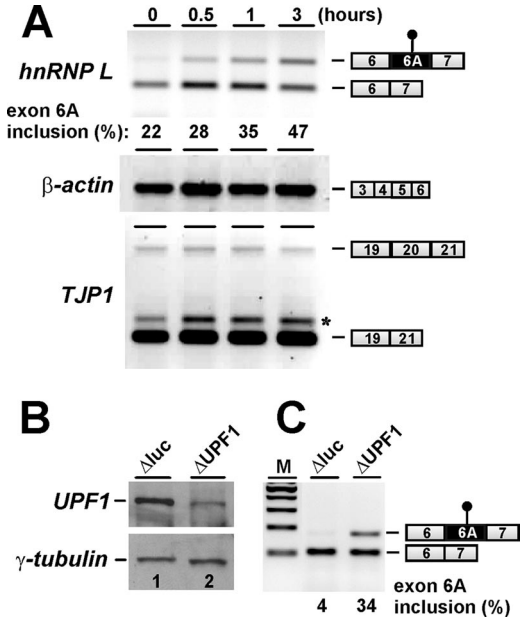

FIG. 2. Exon 6A in the human hnRNP L gene is an NMD target. (A) HnRNP L exon 6A inclusion is increased after cycloheximide treatment. HeLa cells were treated with cycloheximide over 3 h, and total RNA was prepared after 0, 0.5, 1, and 3 h (as indicated) and analyzed by semiquantitative RT-PCR for exon 6A inclusion (top). Quantitation of exon 6A inclusion is given below the lanes (in percentages). The panels below show control RT-PCRs for β-actin mRNA (middle), and for alternative splicing of another hnRNP L target gene, *TJP1* (bottom; the band marked by the asterisk represents a PCR artifact). RT-PCR products are schematically represented on the right. (B and C) hnRNP L exon 6A inclusion is increased after UPF1 knockdown (ΔUPF1). UPF1 expression was downregulated in HeLa cells by RNAi, with a luciferase knockdown (Δluc) as a control (see panel B for Western blot analysis of UPF1 and control γ-tubulin protein levels). (C) Total RNA after knockdowns of UPF1 (ΔUPF1) and control luciferase (Δluc) was analyzed for exon 6A inclusion by RT-PCR (RT-PCR products schematically represented on the right). Quantitation of hnRNP L exon 6A inclusion is given below the lanes (in percentages). M, DNA size markers.

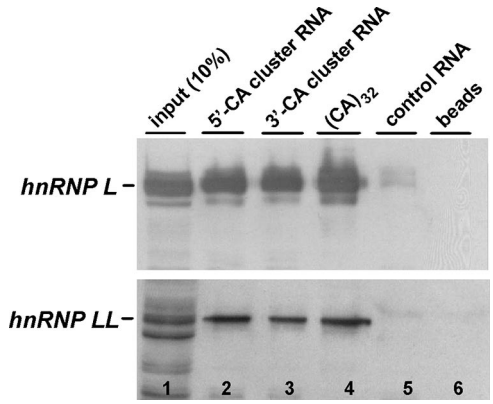

FIG. 3. CA cluster in intron 6 binds hnRNP L, as well as hnRNP LL. Biotinylated 5′ and 3′ parts (lanes 2 and 3, respectively) of the CA cluster of hnRNP L intron 6, as well as biotinylated $(CA)_{32}$ RNA (lane 4) or an unrelated biotinylated control RNA (lane 5), were incubated in HeLa nuclear extract, followed by neutravidin-agarose selection, release of bound protein, and Western blot analysis with anti-hnRNP L monoclonal antibody 4D11 (top panel) or anti-hnRNP LL antibody (bottom panel). In a control reaction, no RNA was added (lane 6). For comparison, 10% of the nuclear extract input was analyzed (lane 1).

CA cluster of the hnRNP L gene, based on the SELEX-derived RNA-binding specificity of hnRNP L (13) and a corresponding scoring system (16) (see Fig. 1C). In vitro binding assays confirmed this (Fig. 3, top panel): the CA cluster RNA was transcribed in two parts, the 5′-terminal portion (300 nt; 5′-CA cluster) and the 3′-terminal portion (346 nt; 3′-CA cluster); both were 3′-biotinylated and incubated in HeLa cell nuclear extract, followed by binding to neutravidin-agarose, washing, release of bound protein, and analysis by Western blotting with an hnRNP L-specific monoclonal antibody, 4D11. As specificity controls, we included a 5′-biotinylated $(CA)_{32}$ RNA oligonucleotide, an unrelated 3′-biotinylated RNA, and beads alone. As a result, both parts of the CA cluster RNA region efficiently bound hnRNP L from nuclear extract (between 5 and 10% of total hnRNP L under these conditions; compare Fig. 3, lanes 1 to 3), comparable to binding to $(CA)_{32}$ RNA (lane 4), whereas a similarly sized control RNA or beads alone did not recover significant hnRNP L amounts (lanes 5 to 6). We conclude that the conserved CA cluster in intron 6 specifically binds hnRNP L.

In parallel, we assayed for binding of the paralog protein hnRNP LL (Fig. 3, bottom panel), which also bound specifically to both parts of the hnRNP L CA cluster, as well as to the $(CA)_{32}$ RNA oligonucleotide (see the Discussion).

hnRNP L protein activates inclusion of its own poison exon 6A. Since hnRNP L binds to the intronic CA cluster upstream of poison exon 6A (Fig. 3), we next tested whether hnRNP L regulates exon 6A usage, using RNAi knockdown, followed by RT-PCR assays of alternative splicing of the endogenous hnRNP L pre-mRNA (Fig. 4A to C). hnRNP L protein levels could be reduced by RNAi to 23% compared to the luciferase control (Fig. 4A). RT-PCR assays under semiquantitative conditions showed that in the absence of cycloheximide the inclusion of exon 6A was almost undetectable (Fig. 4B, lanes 1 and 2), a finding consistent with previous assays (see above). In the presence of cycloheximide, however, when NMD is ineffective, exon 6A is included and significantly reduced after hnRNP L knockdown (Fig. 4B, compare lanes 3 and 4).

We analyzed this finding further in a quantitative manner, using RT/real-time PCR and a panel of different primer pairs across the hnRNP L gene (Fig. 4C). First, downregulation of hnRNP L mRNA after hnRNP L knockdown was measured with the following primer combinations: exons 2 and 3, 4 and 5, 7 and 8, 8 to 10, and 6A and 7, comparing them in each case to the luciferase control knockdown (Fig. 4C). The first four primer combinations gave knockdown values between 23 and 29%, whereas with the exon 6A-7 primer combination a reduction of spliced mRNA to 7% was measured. These values can also be expressed as exon 6A inclusion ratios, comparing the regulated exon 6A to each of the other exons (Fig. 4C, bottom). We conclude that hnRNP L knockdown specifically affects exon 6A inclusion, reducing it to levels of approximately 26 to 32% relative to the other, constitutive exons. This indicates that hnRNP L acts as an activator of its own poison exon 6A, setting up an autoregulatory negative-feedback loop in hnRNP L expression.

In addition, we also examined how endogenous hnRNP L

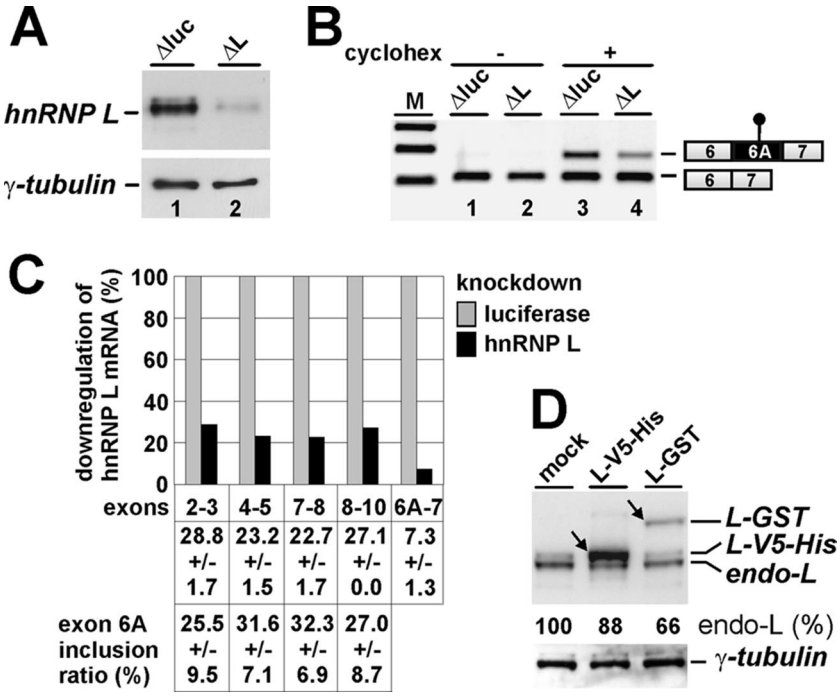

FIG. 4. HnRNP L activates exon 6A inclusion. (A and B) HnRNP L expression was downregulated in HeLa cells by RNAi (ΔL), with luciferase (Δluc) as a control, and hnRNP L and control γ-tubulin protein levels were analyzed by Western blotting (panel A, compare lanes 1 and 2). After UPF1 and control luciferase knockdowns, with (+) or without (−) an additional cycloheximide treatment (cyclohex), total RNA was prepared and exon 6A inclusion was measured by RT-PCR (panel B, lanes 1 to 4; RT-PCR products are schematically represented on the right). M, DNA size markers. (C) RNAi-mediated downregulation of hnRNP L mRNA: real-time RT-PCR analysis. hnRNP L mRNA levels were quantitated after RNAi knockdown, using real-time RT-PCR and primer combinations in exons 2 and 3, 4 and 5, 7 and 8, 8 to 10, or 6A and 7, each normalized to β-actin mRNA levels and in comparison to the luciferase control knockdown (set at 100%; each primer pair was measured twice). Below, the percentages of hnRNP L mRNA downregulation are given, including the standard deviations. In addition, the exon 6A inclusion ratios were determined from these values, each relative to exons 2 and 3, 4 and 5, 7 and 8, or 8 to 10 (the percentages, including standard deviations are shown). (D) HnRNP L overexpression downregulates endogenous hnRNP L protein levels. HeLa cells were transfected with constructs expressing V5-His-tagged hnRNP L (L-V5-His) or GST-tagged hnRNP L (L-GST) or were mock transfected. At 2 days posttransfection endogenous hnRNP L (endo-L), as well as V5-His- and GST-tagged hnRNP L (see arrows), was detected by Western blotting, as well as γ-tubulin as an input control. The levels of endogenous hnRNP L were quantitated as a percentage relative to mock-treated samples and normalized to γ-tubulin levels.

protein levels responded to overexpression of hnRNP L (Fig. 4D). After transient transfection of HeLa cells with hnRNP L expression constructs for V5-His-tagged hnRNP L (L-V5-His) or GST-tagged hnRNP L (L-GST), the hnRNP L levels were analyzed by Western blotting, detecting both endogenous and tagged hnRNP L proteins. Quantitation of endogenous hnRNP L revealed a downregulation of steady-state protein levels to 88 or 66% relative to the mock control, when L-V5-His or L-GST, respectively, were expressed. This finding further supports our conclusion that hnRNP L levels are autoregulated, based on overexpression and on the protein level.

Intronic CA-rich cluster acts as an hnRNP L-dependent splicing enhancer of exon 6A inclusion. Next, we tested directly whether the intronic CA cluster works as an hnRNP L-dependent splicing enhancer of poison exon 6A, using an in vitro alternative splicing assay and hnRNP L depletion and/or complementation. Based on the T7 DUP4-1 plasmid (24), we generated two heterologous constructs that express three-exon pre-mRNAs of 1.2 kb. The first and last exons are β-globin exons 1 and 2, respectively, with a 0.6-kb region inserted in the intron carrying the 3′-terminal part of the hnRNP L CA-cluster and the adjacent exon 6A (T7-DUP 3′CA-cluster-6A [Fig. 5A]). To control for specificity, we also replaced the CA cluster by an unrelated sequence of similar length (T7-DUP control-6A). HeLa nuclear extract was depleted of hnRNP L, using a biotinylated $(CA)_{32}$ RNA oligonucleotide and neutravidin-agarose (15), which removed more than 90% of hnRNP L, compared to mock depletion (see Fig. 5B for the Western blot analysis).

When the heterologous three-exon pre-mRNA with the CA cluster upstream of exon 6A was spliced in mock-depleted nuclear extract, we observed predominantly inclusion of exon 6A (Fig. 5C, lane 8). In contrast, depleting hnRNP L almost completely abolished the exon 6A inclusion product and left the same low level of two-exon product as seen in mock-depleted extract (compare lanes 1 and 8). Add-back of increasing quantities of recombinant hnRNP L restored high levels of exon 6A inclusion (10 to 400 ng of hnRNP L per 25-μl reaction mixture; see Fig. 5C, lanes 2 to 7). Note that 200 ng per 25-μl reaction mixture corresponds to the normal hnRNP L levels in HeLa nuclear extract (16).

To demonstrate that this in vitro splicing activation depends on the CA cluster, we performed the same assays with the T7-DUP control-6A pre-mRNA, which carries instead of the CA cluster an unrelated sequence element upstream of exon 6A (Fig. 5C, lanes 9 to 11). In contrast to the CA cluster

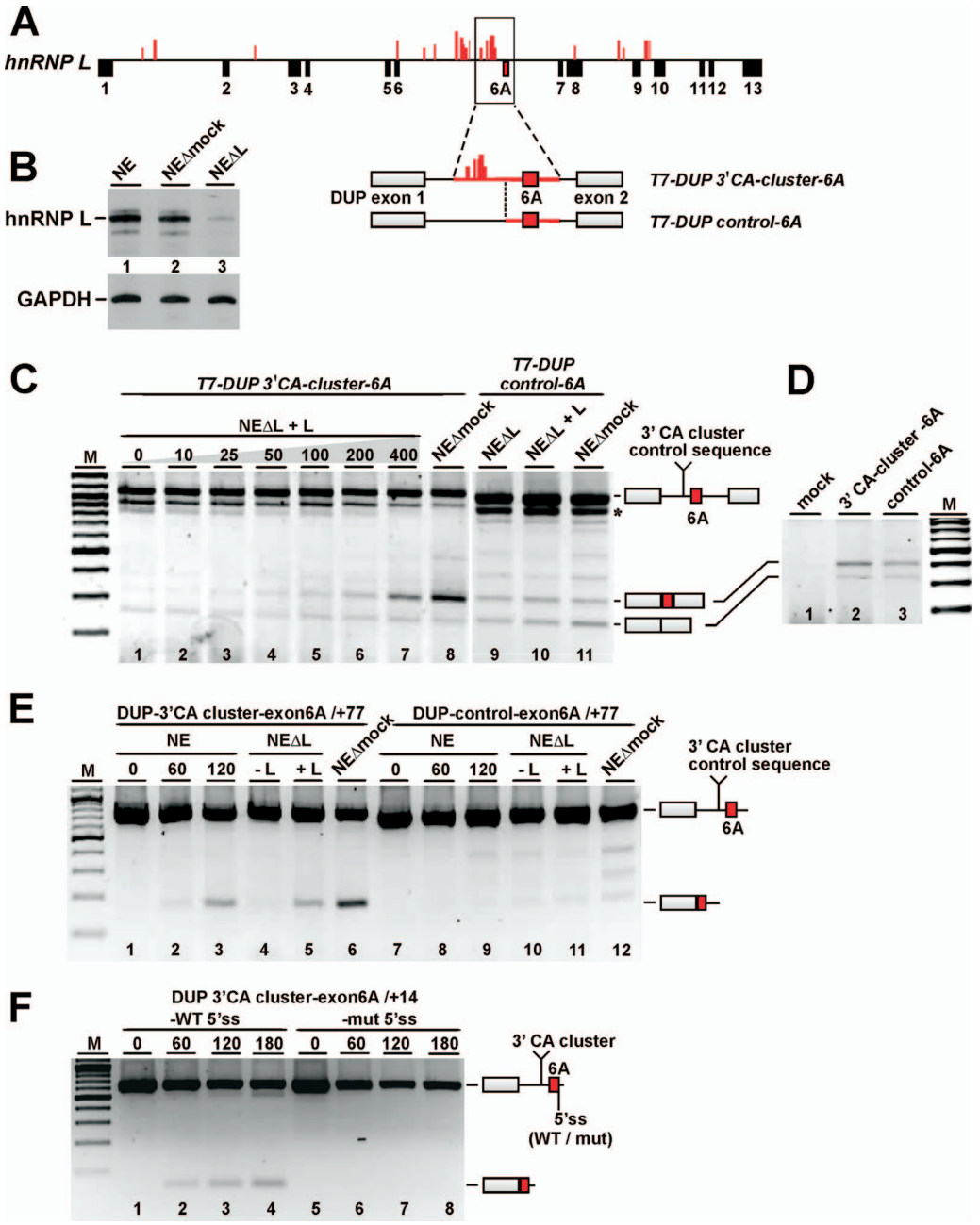

FIG. 5. Intronic CA cluster acts as an hnRNP L-dependent enhancer of hnRNP L exon 6A inclusion. (A) Exon-intron structure of human hnRNP L gene, with the red bars above the line indicating hnRNP L binding motifs (height of bars representing CA richness [16]). The 3′-CA cluster region and exon 6A (boxed area) was inserted in pDUP, to give the heterologous construct T7-DUP 3′-CA cluster-6A. As a control, the 3′-CA cluster was replaced by an unrelated sequence (T7-DUP control-6A). (B and C) HnRNP L- and CA cluster-dependent activation of exon 6A inclusion in vitro. HeLa nuclear extract (NE; panel B, lane 1) was depleted of hnRNP L (NEΔL; see lane 3) or mock depleted (NEΔmock; lane 2) and analyzed by Western blotting with antibody against hnRNP L (panel B, top) or as a control, GAPDH (panel B, bottom). (C) The 3′ CA-cluster-6A pre-mRNA was spliced for 120 min in L-depleted nuclear extract complemented with increasing amounts of recombinant hnRNP L (0 to 400 ng per 25 μl, as indicated; see lanes 1 to 7) or in mock-depleted nuclear extract (lane 8). The control pre-mRNA (control-6A) was spliced in L-depleted extract (NEΔL; lane 9), in L-depleted extract complemented with 200 ng of hnRNP L per 25-μl reaction mixture (NEΔL+L; lane 10), and in mock-depleted extract (NEΔmock; lane 11). Splicing was monitored by RT-PCR, the positions of pre-mRNAs and inclusion/skipping products schematized on the right (the asterisk marks a partially spliced product, with the first intron retained). M, DNA size markers. (D) CA cluster-dependent exon 6A inclusion in vivo. HeLa cells were mock transfected (*mock*; lane 1) or transfected with the 3′-CA cluster-6A construct (lane 2) or with the control-6A construct (lane 3). At 2 days posttransfection total RNA was prepared and analyzed by RT-PCR, monitoring exon 6A inclusion. The positions of inclusion and skipping products are schematized on the left. M, DNA size markers. (E) hnRNP L- and CA cluster-dependent activation of exon 6A inclusion in a two-exon context in vitro. The two-exon pre-mRNAs 3′CA cluster-exon6A/+77 (lanes 1 to 6) or control-exon6A/+77 (lanes 7 to 12), each with 77 nt of intron 6A, were spliced in nuclear extract (NE; for 0, 60, and 120 min, as indicated), in L-depleted (NEΔL; 120 min), or in mock-depleted nuclear extract (NEΔmock; 120 min). For complementation with recombinant hnRNP L (+L), 200 ng of per 25-μl reaction mixture were used. Splicing was monitored by RT-PCR, the positions of pre-mRNAs and spliced product are indicated on the right. M, DNA size markers. (F) Exon 6A recognition depends on intact 5′ splice site. The two-exon pre-mRNAs 3′CA cluster-exon6A/+14 (with 14 nucleotides of intron 6A), carrying a wild-type (lanes 1 to 4) or mutated 5′ splice site (lanes 5 to 8), were spliced in nuclear extract for the times indicated (in minutes). Splicing was monitored by RT-PCR, and the positions of pre-mRNAs and spliced product are indicated on the right. M, DNA size markers.

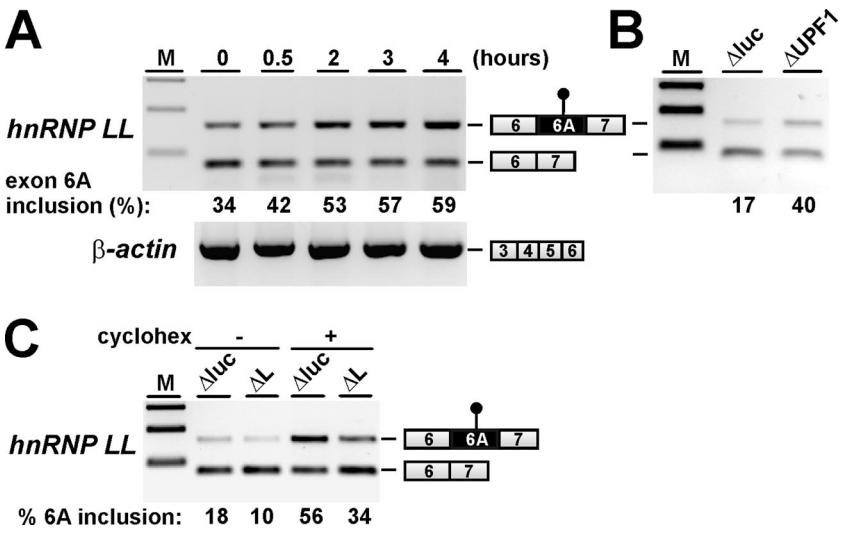

FIG. 6. Cross-regulation of the paralog gene hnRNP LL by hnRNP L. (A and B) Exon 6A in the human hnRNP LL pre-mRNA is an NMD target. (A) hnRNP LL exon 6A inclusion is increased after cycloheximide treatment. HeLa cells were treated with cycloheximide over 4 h, and total RNA was prepared after 0, 0.5, 2, 3, and 4 h (as indicated) and analyzed by semiquantitative RT-PCR for exon 6A inclusion (top) and, as a control, for β-actin mRNA (bottom). RT-PCR products are schematically represented on the right for both panels. (B) hnRNP LL exon 6A inclusion is increased after UPF1 knockdown. UPF1 expression was downregulated in HeLa cells by RNAi (ΔUPF1), with a luciferase knockdown as a control (Δluc). Total RNA after UPF1 and control luciferase knockdowns was analyzed for hnRNP LL exon 6A inclusion by RT-PCR. Quantitation of hnRNP LL exon 6A inclusion is given below the lanes (in percentages). M, DNA size marker. (C) hnRNP L activates hnRNP LL exon 6A inclusion. hnRNP L expression was downregulated in HeLa cells by RNAi (ΔL), with a luciferase knockdown (Δluc) as a control, with (+) or without (−) an additional cycloheximide treatment after knockdown (cyclohex). Total RNA after UPF1 and control luciferase knockdowns was analyzed for hnRNP LL exon 6A inclusion by RT-PCR (products schematically represented on the right). Quantitation of hnRNP LL exon 6A inclusion is given below the lanes (in percentages). M, DNA size markers.

pre-mRNA, exon 6A was included here only to very low levels. Importantly, these levels did not significantly change, whether mock-depleted, hnRNP L-depleted, or hnRNP L-complemented extract was used (compare lanes 9 to 11).

The same two three-exon constructs were also transiently transfected into HeLa cells, in parallel to a mock control in the absence of DNA, and exon 6A splicing was determined by RT-PCR (Fig. 5D). Clearly, exon 6A inclusion increased in the case of the 3′ CA cluster containing construct in comparison with the control pre-mRNA (compare lanes 2 and 3), confirming the in vitro results.

Next, we assayed the enhancer function of the CA cluster in a two-exon context (Fig. 5E). From the heterologous T7-DUP constructs (see above), pre-mRNAs were generated that contained only the first two exons, that is, a β-globin first exon and hnRNP L exon 6A, with the 3′ CA cluster (lanes 1 to 6) or with the control sequence (lanes 7 to 12), and with 77 nt of intronic sequence downstream of exon 6A. Clearly, in vitro splicing of these two heterologous exons strictly depended on the 3′ CA cluster (compare lanes 1 to 3 and lanes 7 to 9; for mock-depleted nuclear extract, compare lanes 6 and 12). Furthermore, complementation assays proved that splicing activity required hnRNP L (compare lanes 4 to 6).

Finally, we sought to determine whether the enhancer effect of the CA cluster requires an intact exon 6A (Fig. 5F). A two-exon pre-mRNA was assayed by in vitro splicing that contained the β-globin first exon and the hnRNP L exon 6A, including the 3′ CA cluster, but only 14 nt of intron 6A, with the normal 5′ splice site of exon 6A (-WT 5'ss; lanes 1 to 4) or a mutated 5′ splice site (-mut 5'ss; lanes 5 to 8), in which the GU dinucleotide was deleted. RT-PCR assays demonstrated that splicing of these two-exon pre-mRNAs required a functional 5′ splice site of exon 6A, indicating that this 5′ splice site is necessary for exon definition.

In sum, this provided direct biochemical evidence that hnRNP L is responsible and sufficient for exon 6A activation, whereby the CA cluster plays an essential role as an intronic splicing enhancer element.

hnRNP LL: autoregulation of the paralog gene and cross-regulation by hnRNP L. We have recently described the hnRNP LL protein, which is closely related in domain structure and sequence to the classical hnRNP L (16). In that study we had also observed that, upon hnRNP L knockdown, hnRNP LL was upregulated at both mRNA and protein levels, suggesting a cross-regulatory mechanism. Therefore, we first compared the exon-intron organization of the human and mouse hnRNP LL gene and analyzed nucleotide sequence conservation across vertebrate species (see Fig. S2 in the supplemental material). Surprisingly, we noted in the hnRNP LL gene—as described above for the hnRNP L gene (Fig. 1)—an extended, highly conserved region spanning at least 1.5 kb in hnRNP LL intron 6. Strikingly, within this region we found a potential poison exon of 83 nt (cDNA AL 512692), which was not part of the RefSeq mRNA and which we called exon 6A.

Whether the hnRNP LL exon 6A is NMD responsive, we tested again by cycloheximide treatment, as well as after UPF1 knockdown (Fig. 6A and B, respectively). In contrast to hnRNP L (see Fig. 2), in the case of the hnRNP LL gene exon 6A was readily detectable in steady-state RNA from HeLa cells (Fig. 6A, time point zero). Inclusion of hnRNP LL exon 6A

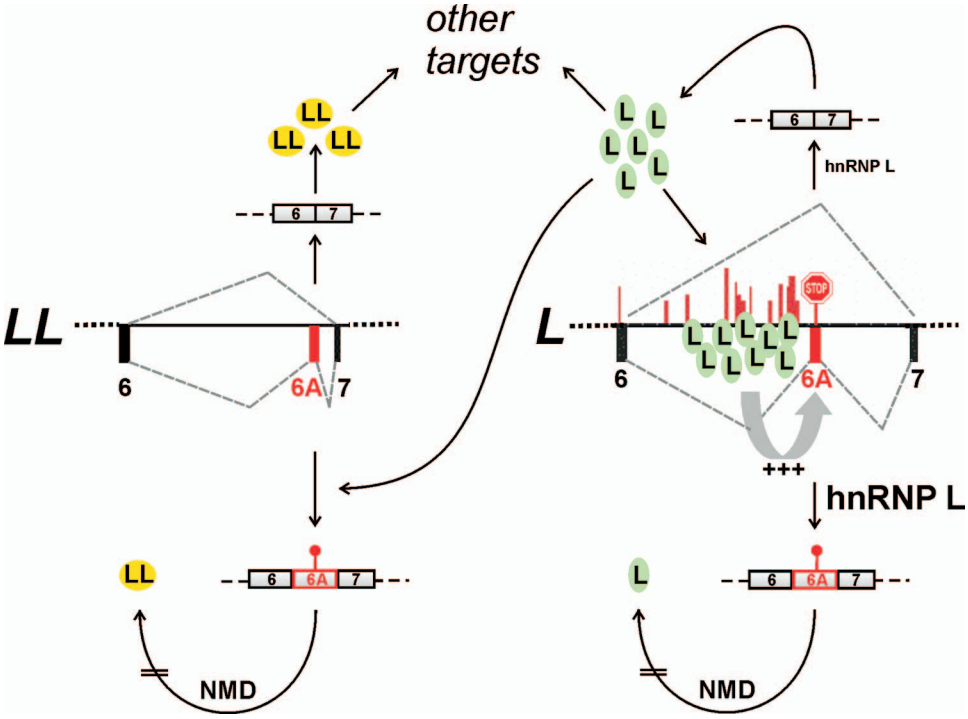

FIG. 7. Model of hnRNP L auto- and cross-regulation. The hnRNP L pre-mRNA can switch in its exon 6-7 region between two alternative splicing modes (right part of the figure). First, at low hnRNP L levels, exon 6A is skipped, resulting in functional hnRNP L mRNA and thereby increasing L protein levels (top). Second, at high levels hnRNP L binds to the intronic CA-cluster enhancer, promoting exon 6A inclusion, which results in NMD-mediated downregulation of hnRNP L expression (bottom). This hnRNP L-dependent switch creates an autoregulatory feedback mechanism, which contributes to hnRNP L homeostasis. In addition, hnRNP L regulates diverse alternative splicing processes in many other target genes (13, 16), among them (see left part of figure) the paralog gene hnRNP LL, which contains an analogous poison exon 6A that also switches, depending on hnRNP L—between inclusion and skipping. Finally, hnRNP LL targets many alternative splicing processes in a cell-type-specific manner (27).

strongly increased after cycloheximide treatment over 4 h (from 34 to 59%; see Fig. 6A) and also by UPF1 knockdown (40%, compared to 17% in the luciferase control; see Fig. 6B). We conclude that exon 6A inclusion in splicing of the paralog hnRNP LL pre-mRNA does induce NMD.

Since in our previous study we had described reciprocal cross-regulation of hnRNP LL expression by hnRNP L (16), we considered that this effect might be mediated though regulation of exon 6A inclusion. Therefore, exon 6A inclusion levels were measured by semiquantitative RT-PCR, comparing HeLa cells after luciferase or hnRNP L knockdown (Fig. 6C). To enhance a potential effect, we assayed also after cycloheximide treatment to inactivate NMD. Clearly, hnRNP LL exon 6A inclusion strongly decreased after hnRNP L downregulation (from 56 to 34% in the presence of cycloheximide), an effect we could even detect in the absence of cycloheximide (from 18 to 10%). In sum, this demonstrates that hnRNP L activates exon 6A inclusion in hnRNP LL splicing, a cross-regulatory mechanism, which explains the reciprocal regulation of these two closely related hnRNP proteins.

DISCUSSION

Auto- and cross-regulatory network of hnRNP L. Figure 7 summarizes our model of hnRNP L auto- and cross-regulation. hnRNP L autoregulates its own expression on the level of alternative splicing, using a highly conserved, dense, bipartite cluster of CA-rich motifs spread over 800 nt of intron 6, which is followed by a short poison exon (exon 6A; indicated in red). Excess hnRNP L binds with high affinity and specificity to both CA clusters, thereby activating exon 6A inclusion. If included, a premature termination codon is introduced into the mRNA, resulting in NMD and downregulation of functional hnRNP L mRNA levels. Thereby the CA cluster acts as an unusually extended, intronic enhancer of exon 6A inclusion, depending on bound hnRNP L. Note that the 3′ splice site of exon 6A is extremely low in quality and contains no recognizable pyrimidine tract (MaxEntScan score of 1.9 [41]). In sum, excess hnRNP L levels downregulate L expression on the level of alternative splicing and NMD.

This model is based on the following lines of evidence. First, we have shown by both UPF1 knockdown and cycloheximide treatment in HeLa cells that exon 6A is NMD sensitive (Fig. 2). Second, both parts of the CA-rich cluster efficiently and specifically bind hnRNP L in vitro (Fig. 3). Third, as shown by hnRNP L knockdown and real-time PCR analysis, exon 6A inclusion depends on hnRNP L protein levels. In addition, hnRNP L overexpression downregulates endogenous hnRNP L (Fig. 4). Fourth, direct biochemical evidence for an activator role of hnRNP L and the enhancer function of the CA cluster came from in vitro splicing data in hnRNP L-depleted extract and complementation by recombinant protein (Fig. 5). Finally,

the unusual, very high conservation over almost 2 kb of intron 6 is consistent with an important regulatory function (Fig. 1).

Not only the high level of conservation but also the length of the CA-cluster enhancer in this case is surprising and puzzling, considering that short binding sites for single activators or repressors are normally sufficient for regulation. The human hnRNP L CA cluster consists of two parts of approximately 280 (5′) and 330 (3′) nt, each containing 11 and 14 CA motifs, respectively. Most of these CA motifs are conserved between human and mouse, and the two cluster parts are separated by a region of approximately 215 nt without CA motifs (see Fig. S1 in the supplemental material). Very likely multiple hnRNP L molecules bind to each of the cluster parts, and this may induce a large-scale structural change in the pre-mRNA, involving interactions between several hnRNP L molecules. It is conceivable that the role of multiple L binding sites is to allow a range of conformational changes, sensing the L concentration through different oligomeric complexes and generating an L concentration-dependent splice-regulatory signal.

How does this autoregulatory mechanism compare with the PTB case, a well-characterized example among the splicing factors for this type of regulation?

First, both hnRNP L (as well as the paralogous hnRNP LL) and PTB use NMD to autoregulate their own expression. In hnRNP L, inclusion of the poison exon 6A introduces the premature stop codon, whereas in PTB, it is skipping of exon 11, which leads to loss of the open reading frame. Second, to activate NMD and downregulate gene expression, excess hnRNP L works as an activator of poison exon 6A, whereas PTB represses exon 11, which is part of the normal, functional mRNA. Note that the activator role of hnRNP L demonstrated here contrasts with the usual situation that hnRNP proteins repress from intronic sites, and SR proteins activate from exonic enhancers (for example, see reference 26). Third, both hnRNP L and PTB share that they function through highly conserved intronic sequences, involving multiple binding sites spread over hundreds of nucleotides. Therefore, it is likely they both operate through large oligomeric RNP structures and perhaps multiple conformations.

What is the biological function of this type of autoregulation? As already pointed out by earlier general studies (17, 26), homeostasis of splicing factor levels is certainly a critical feature; for example, we know from early studies that the quantitative ratio between two antagonistic splicing regulators, such as ASF/SF2 and hnRNP A1, can determine the outcome of alternative splicing regulation (5, 22). We have recently determined the protein levels of hnRNP L and its paralog hnRNP LL in HeLa cells (16). Compared to hnRNP LL, hnRNP L is present at approximately tenfold-higher overall concentrations in the cell and, considering nuclear levels, the difference would be even higher. Therefore, hnRNP LL appears to be much more in the repressed state. Consistent with this, the hnRNP LL poison exon can be detected at relatively high levels (Fig. 6A), in contrast to the situation in the hnRNP L pre-mRNA, where poison exon 6A can be detected only after NMD inactivation (Fig. 2). Note that this applies to HeLa cells. In other cell types the relative distribution of hnRNP L versus hnRNP LL appears to be different (S. Schreiner, M. Preussner, and A. Bindereif, unpublished data); this includes also T lymphocytes (27, 38). Additional factors and/or regulatory mechanism on other levels may also come into play, such as translational and miRNA-mediated control.

In addition to autoregulation, hnRNP L targets many other pre-mRNAs, and we have previously identified some of these (13, 16). Here, we have characterized as an additional target of hnRNP L the hnRNP LL pre-mRNA, which is particularly interesting, since both hnRNPs share many features of protein domain structure, as well as the exon-intron structure of their genes (compare Fig. 1 and Fig. S2 in the supplemental material). We have recently reported a cross-regulatory relationship between these two closely related genes: upon hnRNP L knockdown, hnRNP LL was upregulated at both mRNA and protein levels (16). Based on comparing the gene structure and conservation of hnRNP L and LL, we have described here that the analogous poison exon 6A of the hnRNP LL pre-mRNA is activated by hnRNP L (Fig. 6), providing a mechanistic explanation of the cross-regulation observed previously. We did consider examining the reciprocal relationship, i.e., the question whether hnRNP LL cross-regulates hnRNP L, but at least in the HeLa cell system, this may not be biologically meaningful, since nuclear LL protein levels are more than 10-fold below those of hnRNP L (16). Perhaps only in other cell lines or in certain tissues, such as activated T lymphocytes where hnRNP LL regulates CD45 alternative splicing (27, 38), this reciprocal regulation may become relevant. Consistent with this potential cross-regulation, the hnRNP LL protein does bind in vitro to the CA cluster of the hnRNP L pre-mRNA (Fig. 3).

ACKNOWLEDGMENTS

We thank Gideon Dreyfuss for anti-hnRNP L monoclonal antibody 4D11, Niels Gehring and Andreas Kulozik for anti-UPF1 antibody, Jan Medenbach for essential help in qPCR analysis, Karl Stangl for genomic DNA, and other members of our group for helpful discussions and comments on the manuscript.

This study was supported by grants from the Deutsche Forschungsgemeinschaft (DFG grant Bi 316/10), the Federal Ministry for Education and Research (BMBF NGNF-2 program), the European Commission-funded Network of Excellence EURASNET, and the Fonds der Chemischen Industrie.

REFERENCES

1. **Ben-Dov, C., B. Hartmann, J. Lundgren, and J. Valcárcel.** 2008. Genome-wide analysis of alternative pre-mRNA splicing. J. Biol. Chem. **283:**1229–1233.
2. **Black, D. L.** 2003. Mechanisms of alternative pre-messenger RNA splicing. Annu. Rev. Biochem. **72:**291–336.
3. **Blencowe, B. J.** 2006. Alternative splicing: new insights from global analyses. Cell **126:**37–47.
4. **Boutz, P. L., G. Chawla, P. Stoilov, and D. L. Black.** 2007. MicroRNAs regulate the expression of the alternative splicing factor nPTB during muscle development. Genes Dev. **21:**71–84.
5. **Cáceres, J. F., S. Stamm, D. M. Helfman, and A. R. Krainer.** 1994. Regulation of alternative splicing in vivo by overexpression of antagonistic splicing factors. Science **265:**1706–1709.
6. **Cartegni, L., S. L. Chew, and A. R. Krainer.** 2002. Listening to silence and understanding nonsense: exonic mutations that affect splicing. Nat. Rev. Genet. **3:**285–298.
7. **Coutinho-Mansfield, G. C., Y. Xue, Y. Zhang, and X. D. Fu.** 2007. PTB/nPTB switch: a posttranscriptional mechanism for programming neuronal differentiation. Genes Dev. **21:**1573–1577.
8. **Gehring, N. H., J. B. Kunz, G. Neu-Yilik, S. Breit, M. H. Viegas, M. W. Hentze, and A. E. Kulozik.** 2005. Exon-junction complex components specify distinct routes of nonsense-mediated mRNA decay with differential cofactor requirements. Mol. Cell **20:**65–75.
9. **Guang, S., A. M. Felthauser, and J. E. Mertz.** 2005. Binding of hnRNP L to the pre-mRNA processing enhancer of the herpes simplex virus thymidine kinase gene enhances both polyadenylation and nucleocytoplasmic export of intronless mRNAs. Mol. Cell. Biol. **25:**6303–6313.

10. **Hahm, B., Y. K. Kim, J. H. Kim, T. Y. Kim, and S. K. Jang.** 1998. Heterogeneous nuclear ribonucleoprotein L interacts with the 3′ border of the internal ribosomal entry site of hepatitis C virus. J. Virol. **72:**8782–8788.
11. **Hamilton, B. J., X. W. Wang, J. Collins, D. Bloch, A. Bergeron, B. Henry, B. M. Terry, M. Zan, A. J. Mouland, and W. F. Rigby.** 2008. Separate cis-trans pathways post-transcriptionally regulate murine CD154 (CD40 ligand) expression: a novel function for CA repeats in the 3′ untranslated region. J. Biol. Chem. **283:**25606–25616.
12. **House, A. E., and K. W. Lynch.** 2006. An exonic splicing silencer represses spliceosome assembly after ATP-dependent exon recognition. Nat. Struct. Mol. Biol. **13:**937–944.
13. **Hui, J., L.-H. Hung, M. Heiner, S. Schreiner, N. Neumüller, G. Reither, S. A. Haas, and A. Bindereif.** 2005. Intronic CA-repeat and CA-rich elements: a new class of regulators of mammalian alternative splicing. EMBO J. **24:** 1988–1998.
14. **Hui, J., G. Reither, and A. Bindereif.** 2003. Novel functional role of CA repeats and hnRNP L in RNA stability. RNA. **9:**931–936.
15. **Hui, J., K. Stangl, W. L. Lane, and A. Bindereif.** 2003. HnRNP L stimulates splicing of the eNOS gene by binding to variable-length CA repeats. Nat. Struct. Biol. **10:**33–37.
16. **Hung, L.-H., M. Heiner, J. Hui, S. Schreiner, V. Benes, and A. Bindereif.** 2008. Diverse roles of hnRNP L in mammalian mRNA processing: a combined microarray and RNAi analysis. RNA. **14:**284–296.
17. **Lareau, L. F., M. Inada, R. E. Green, J. C. Wengrod, and S. E. Brenner.** 2007. Unproductive splicing of SR genes associated with highly conserved and ultraconserved DNA elements. Nature **446:**926–929.
18. **Liu, X., and J. E. Mertz.** 1995. hnRNP L binds a *cis*-acting RNA sequence element that enables intron-independent gene expression. Genes Dev. **9:**1766–1780.
19. **Makeyev, E. V., and T. Maniatis.** 2008. Multilevel regulation of gene expression by microRNAs. Science **319:**1789–1790.
20. **Makeyev, E. V., J. Zhang, M. A. Carrasco, and T. Maniatis.** 2007. The microRNA miR-124 promotes neuronal differentiation by triggering brain-specific alternative pre-mRNA splicing. Mol. Cell **27:**435–448.
21. **Matlin, A. J., F. Clark, and C. W. Smith.** 2005. Understanding alternative splicing: toward a cellular code. Nat. Rev. Mol. Cell. Biol. **6:**386–398.
22. **Mayeda, A., and A. R. Krainer.** 1992. Regulation of alternative pre-mRNA splicing by hnRNP A1 and splicing factor SF2. Cell **68:**365–375.
23. **Melton, A. A., J. Jackson, J. Wang, and K. W. Lynch.** 2007. Combinatorial control of signal-induced exon repression by hnRNP L and PSF. Mol. Cell. Biol. **27:**6972–6984.
24. **Modafferi, E. F., and D. L. Black.** 1997. A complex intronic splicing enhancer from the c-src pre-mRNA activates inclusion of a heterologous exon. Mol. Cell. Biol. **17:**6537–6545.
25. **Modrek, B., and C. Lee.** 2002. A genomic view of alternative splicing. Nat. Genet. **30:**13–19.
26. **Ni, J. Z., L. Grate, J. P. Donohue, C. Preston, N. Nobida, G. O'Brien, L. Shiue, T. A. Clark, J. E. Blume, and M. Ares, Jr.** 2007. Ultraconserved elements are associated with homeostatic control of splicing regulators by alternative splicing and nonsense-mediated decay. Genes Dev. **21:**708–718.
27. **Oberdoerffer, S., L. F. Moita, D. Neems, R. P. Freitas, N. Hacohen, and A. Rao.** 2008. Regulation of CD45 alternative splicing by heterogeneous ribonucleoprotein, hnRNP LL. Science **321:**686–691.
28. **Pan, Q., A. L. Saltzman, Y. K. Kim, C. Misquitta, O. Shai, L. E. Maquat, B. J. Frey, and B. J. Blencowe.** 2006. Quantitative microarray profiling provides evidence against widespread coupling of alternative splicing with nonsense-mediated mRNA decay to control gene expression. Genes Dev. **20:**153–158.
29. **Piñol-Roma, S., M. S. Swanson, J. G. Gall, and G. Dreyfuss.** 1989. A novel heterogeneous nuclear RNP protein with a unique distribution on nascent transcripts. J. Cell Biol. **109:**2575–2587.
30. **Rothrock, C. R., A. E. House, and K. W. Lynch.** 2005. HnRNP L represses exon splicing via a regulated exonic splicing silencer. EMBO J. **24:**2792–2802.
31. **Saltzman, A. L., Y. K. Kim, Q. Pan, M. M. Fagnani, L. E. Maquat, and B. J. Blencowe.** 2008. Regulation of multiple core spliceosomal proteins by alternative splicing-coupled nonsense-mediated mRNA decay. Mol. Cell. Biol. **28:**4320–4330.
32. **Sambrook, J., E. F. Fritsch, and T. Maniatis.** 1989. Molecular cloning: a laboratory manual, 2nd ed. Cold Spring Harbor Laboratory Press, Cold Spring Harbor, NY.
33. **Shih, S. C., and K. P. Claffey.** 1999. Regulation of human vascular endothelial growth factor mRNA stability in hypoxia by heterogeneous nuclear ribonucleoprotein L. J. Biol. Chem. **274:**1359–1365.
34. **Shin, C., and J. L. Manley.** 2004. Cell signalling and the control of pre-mRNA splicing. Nat. Rev. Mol. Cell. Biol. **5:**727–738.
35. **Shur, I., D. Ben-Avraham, and D. Benayahu.** 2004. Alternatively spliced isoforms of a novel stromal RNA regulating factor. Gene **334:**113–121.
36. **Smith, C. W., and J. Valcárcel.** 2000. Alternative pre-mRNA splicing: the logic of combinatorial control. Trends Biochem. Sci. **25:**381–388.
37. **Spellman, R., M. Llorian, and C. W. Smith.** 2007. Crossregulation and functional redundancy between the splicing regulator PTB and its paralogs nPTB and ROD1. Mol. Cell **27:**420–434.
38. **Topp, J. D., J. Jackson, A. A. Melton, and K. W. Lynch.** 2008. A cell-based screen for splicing regulators identifies hnRNP LL as a distinct signal-induced repressor of CD45 variable exon 4. RNA **14:**2038–2049.
39. **Willkomm, D. K., and R. K. Hartmann.** 2005. 3′-Terminal attachment of fluoroescent dyes and biotin, p. 86–94. *In* E. Westhof, A. Bindereif, A. Schön, and R. K. Hartmann (ed.), Handbook of RNA biochemistry. Wiley-VCH, New York, NY.
40. **Wollerton, M. C., C. Gooding, E. J. Wagner, M. A. Garcia-Blanco, and C. W. Smith.** 2004. Autoregulation of polypyrimidine tract binding protein by alternative splicing leading to nonsense-mediated decay. Mol. Cell **13:**91–100.
41. **Yeo, G., and C. B. Burge.** 2004. Maximum entropy modeling of short sequence motifs with applications to RNA splicing signals. J. Comp. Biol. **11:**377–394.